Effect of melting conditions on striae in iron-bearing silicate melts

Jensen, Martin; Yue, Yuanzheng

Published in:
European Journal of Glass Science and Technology Part A

Publication date:
2012

Document Version
Early version, also known as pre-print

Glass Technol.: Eur. J. Glass Sci. Technol. A, February 2012, **53** (1), 20–28

Effect of melting conditions on striae in iron-bearing silicate melts

Martin Jensen & Yuanzheng Yue[1]

Section of Chemistry, Aalborg University, 9000 Aalborg, Denmark

Manuscript received 18 August 2011
Revision received 18 October 2011
Manuscript accepted 6 November 2011

Chemical striae are present in a broad range of glass products, but due to their negative impact on for example the optical and mechanical properties, elimination of striae from melts is a key issue in glass technology. By varying melting temperatures, retention times and redox conditions of an iron-bearing calcium aluminosilicate melt, we quantify the effect of each of the three melting parameters on the stria content in the melt. The quantification of the stria content in the melt is conducted by means of image analysis on cast melt samples. We find that in comparison to an extension of retention time an increase of melt temperature and/or a decrease of viscosity play a more important role in decreasing the stria content. We also demonstrate that the extent of striation is influenced by the crucible materials that cause a change of redox state of the melt, and hence its viscosity. We discuss the effect of other factors such as compositional fluctuation of the melt and bubbling due to iron reduction on the stria content. During the melting process, striae with a chemical gradient in a more mobile species equilibrate faster than striae caused by a chemical gradient in a less mobile species. The temperature and time effects on melt homogeneity at lower temperatures are larger than at higher temperatures.

1. Introduction

Most oxide glasses are produced by melting a batch composed of various raw materials in a furnace and subsequently casting the melt after a certain retention period in the furnace at a given temperature. During the melting process, several physical and chemical reactions occur, for example incorporation of atmospheric air into the glass melt, degassing of CO_2 from carbonates in the raw materials, and chemical dissolution of the raw materials in the glass melt. To avoid undesired species such as bubbles, undissolved stones and striae, a retention period is needed during the melting process. Removal of such species from the glass melts is crucial as they negatively affect the mechanical properties of the final glass product.[1–3] The chemical differences between the various raw materials lead to chemical striae in the melt if the homogenisation process is incomplete, i.e. the homogenisation temperature and retention time are insufficient. A stria is a glassy domain within the glass matrix which has a composition gradient from the surrounding glass. A gradual elimination of chemical striae continuously takes places during diffusion when the temperature of the melt is above the liquidus temperature. The diffusion process is driven by an entropy increase of the melt in accordance with the second law of thermodynamics. At the interface between the striated domain and the melt matrix there is diffusion of the species that are enriched or depleted in the stria. Therefore, complete elimination of a stria in the melt requires that the diffusion length of the species in question is at least half the stria dimension. Elimination of striae in glass melts is a complex issue affected by several factors such as melting temperature, retention time and the grain size of the raw materials. The grain size determines the size of the chemical striae after the batch has entered the molten state.

Due to its scientific and technological importance, striae elimination has been a major topic of glass research over many years.[4–11] Because of the increasing composition gradient of one or more species from the glass matrix to the centre of the stria, there is no well defined boundary between the stria and the glass matrix. The lack of a clear boundary complicates the quantification of striae in glasses. However, very recently, a simple and accurate approach for stria characterisation has been established based on image processing[12,13] and has been proved to be applicable to a wide range of glasses .[14] In the present study, we use this approach to investigate the equilibration of stria in an iron-bearing calcium aluminosilicate melt, i.e. a basalt-like composition, by varying melting conditions such as melting temperature and retention time. This melt composition is often used for production of stone wool; a mineral wool used for insulation. Monitoring and elimination of striae in the melt is essential for assuring both an efficient production process and a high quality glass product. This study also provides insight into the sources of formation of striae in glass and indirectly gives information on how to remove striae from glass melts in general. Furthermore, we investigate the influence of the melt viscosity on the homogenisation rate by varying the

[1] Corresponding author. Email yy@bio.aau.dk

redox conditions of the melt and thereby the oxidation state of iron, and hence the melt viscosity.

2. Experimental

2.1. Raw materials

The glass batch was produced from raw materials used in industrial production of stone wool. The batch consisted of two different basalts denoted TAP and Radlovac and a briquette with different raw materials crushed to a size of ~5 mm and embedded in a cement matrix. The raw materials in the briquette included predominantly basalt, dolomite, bauxite and stone wool waste material. The glass batch consisted of three different components with the following masses: 0·5 kg TAP, 2·0 kg Radlovac, and 2·5 kg briquette. The two basalts were cut to a size of about 2×2×2 cm^3. The briquettes were added as pieces with a size around 3×3×3 cm^3. The chemical composition of the raw materials and of the entire batch is provided in Table 1. Using the Bottinga–Weill model,[15] a melt with the same chemical composition as the batch is found to have a viscosity of 4·9, 2·7, 1·8 and 1·1 Pa s at 1300, 1350, 1400 and 1450°C, respectively, when iron is present in its ferrous state. For one experiment, the two basalts were added as slices with a thickness of 2 cm and an area of about 10×7cm^2. In addition to one batch, 100 g of 5 mm coke pieces were added.

2.2. Glass melting setup

The glass melts were produced in a 7 L Mars uniC-star XO 40 SiC crucible doped with graphite (Aug. Gundlach, Germany). The crucible is conducting and exposes the melt to reducing conditions since it contains graphite. The conducting properties of the crucible are important as the melts were produced in an induction furnace. The experimental setup is sketched in Figure 1 and was constructed as follows. The outer surface of the crucible was covered with an Al_2O_3 needle blanket to reduce the thermal radiation from the crucible. The isolated crucible stood on a SiO_2–Al_2O_3 concrete tile placed in a water cooled copper coil connected to a TruHeat MF5040 (Hüttinger Germany) 40 kW generator operating at 44 kHz. The temperature of the crucible was measured by an Infratherm ISQ5 pyrometer (Impac, Germany) through a hole in the Al_2O_3 needle blanket covering the crucible. The pyrometer was connected

Table 1. Chemical composition in wt % of the raw materials and the entire batch. The names TAP and Radlovac refer to two different basalts. All iron oxide is reported as Fe_2O_3

	SiO_2	Al_2O_3	TiO_2	Fe_2O_3	CaO	MgO	Na_2O	K_2O
TAP	49·3	15·8	2·1	11·3	8·5	7·2	3·6	2·3
Radlovac	52·4	16·1	2·0	10·0	9·1	5·8	3·6	0·9
Briquette	28·4	19·3	1·2	11·1	27·5	10·5	1·4	0·6
Batch	40·1	17·7	1·6	10·7	18·2	8·3	2·5	0·9

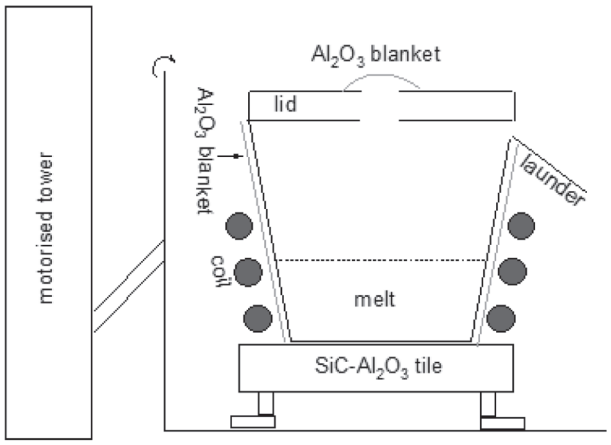

Figure 1. Schematic diagram of the experimental setup used in the production of the glass melts

to a Eurotherm 2408 controller for adjustment of the temperature. The crucible was covered with a lid of the same material as the crucible. An opening was cut in the lid to allow additions of raw materials to the crucible. During the melting experiments, the opening in the crucible was covered with a piece of Al_2O_3 blanket. Prior to the first usage of the crucible, the empty crucible was heated with the lid to 1300°C which burnt out organic additives in the crucible and welded the lid to the crucible. Casting of the melt was achieved by attaching the melt setup to a motorised tower which was used to tilt the crucible and the generator. Furthermore, the tilting mechanism ensures that the crucible is heated during the entire casting process. A GR launder (AUG Gundlach, Germany) was attached to the lip of the melting crucible. To cast the glass melt, the melt setup was tilted and the melt flowed through the launder onto a graphite coated stainless steel table. The graphite coating prevented sticking of the glass to the steel table. To enhance the cooling rate of the glass, the melt was pressed with a graphite coated steel pad.

2.3. Glass production

The batch was added to the SiC crucible at room temperature and the temperature of the crucible was then raised to 1100°C where the raw materials was allowed to equilibrate for approximately 15 min. This thermal equilibration was carried out to ensure uniform experimental conditions. After the temperature equilibration of the batch, the temperature was raised to 1300, 1350, 1400 or 1450°C at a rate of 20°C/min. The melt was kept at the maximum temperature for 10, 20 or 40 min and was then cast on to a graphite coated stainless steel table and pressed with the graphite coated stainless steel plate. Finally, to remove stresses in the glasses, they were transferred to an annealing furnace at 675°C (around the glass transition temperature), and subsequently the furnace was turned off so that the glass naturally cooled to room temperature.

To investigate the influence of the melt viscosity on the stria elimination rate, a Cr_2O_3 refractory paste (RHI AG, Germany) was applied on the inside of the crucible surface. The Cr_2O_3 paste prevented contact between the melt and the reducing graphite in the crucible material, i.e. the redox conditions became more oxidised when the Cr_2O_3 paste was applied. Melts were produced at 1400 °C in the Cr_2O_3 coated crucible in a similar manner to that described above.

2.4. Sample preparation

The resulting glass blocks were cut into pieces about 3×3 mm^2 in size with a diamond coated blade using a Sectocom saw (Struers, Denmark). After cutting, the samples were ground co-parallel to a thickness of 300–350 μm on a cast iron disk using water suspended SiC powder with ISO/FEPA grit sizes of 80, 220, 400, 800 and 1200. The samples were ground to a thickness of 300–400 μm. The samples must be made thin enough to enable sufficient optical transmission through the glass for reasonable image analysis. The optical transmission of the glass in the visible light wavelength region is drastically lowered since the sample contains about 2–6 wt% iron oxide. The polishing in the first step was carried out on an MD Plan cloth (Struers, Denmark) with 9 μm diamond paste and the last step was on another MD Plan cloth with 3 μm CeO_2 humidified with water. Five glass pieces were prepared from each melt.

2.5. Striae characterisation

The striae in the glass pieces were analysed by means of image analysis, which has been shown to be an effective method to characterise striae in various glasses.[12,14] To acquire an image, the sample was placed on a transparent foil in an Epson Perfection V700 Photo scanner (Seiko Epson Corporation, Nagano, Japan). The images were acquired in 8 bit mode at 3200 dots per inch (dpi) and at a brightness of 75 and a contrast of 45. During the scanning procedure, the transmission of the glass was automatically converted to a grey value, which is proportional to the optical transmission. In eight bit mode, the grey value is an integer between 0 and 255. This implies that 2·5 grey values cover 1% change in absolute optical transmission, however, by optimising the brightness and contrast only transmission levels between 10 and 60% were selected for this study. By limiting the investigated optical transmission range, 1% change in optical transmission is covered by five grey values, i.e. optimisation of brightness and contrast for the sample in question improves the detection limit of the method. To reconvert the grey value into an absolute optical transmission an IT8 T070408 standard calibration sheet was utilised (LaserSoft Imaging). To account for differences in sample thickness, l, normalisation was carried out using the Lambert–Beer law.

$$T=10^{-\varepsilon lc} \quad (1)$$

where T is the optical transmission, ε is the extinction coefficient and c is the relative stria concentration. ε is a composition dependent constant. To determine the relative stria concentration from the Lambert-Beer law, the extinction coefficient was set to unity. As the chemical origin can be different for each stria, the extinction coefficient fluctuates across the glass. However, as the species that is enriched in one stria must be depleted in another, a symmetric distribution of the extinction coefficient around a mean value exists. Therefore, it is reasonable to assume a fixed extinction coefficient. Consequently, the relative stria concentration is suppressed in some regions of the glass whereas it is enhanced in others, but the average stria concentration of the glass is unaffected by the assumption.

All prepared glass samples contained bubbles. Similar to striae, bubbles have a contrast difference to the surrounding glass matrix on the acquired images. Therefore, bubbles are detected as very intense striations. Hence, bubbles significantly influence the striae characterisation and were therefore removed from the acquired image through picture processing as described in a previous publication.[13]

The grey values of the image were recorded through line scanning in the software ImageJ.[16] During the line scanning, a line with a length of 2500 pixels (19·85 mm) was inserted on the image and the grey value of every pixel of the line was recorded. Through the recalibration of the grey value to the optical transmission and application of the Lambert-Beer law, the relative stria concentration of each individual pixel on the line was determined. For each sample, 500 lines scans on randomly selected spots were conducted. The 500 line scans were imported into the program Qtiplot and subjected to Fourier transformation and subsequently averaged. Finally, the Fourier transformation spectrum was integrated over stria dimension.

2.6. X-ray fluorescence

A few grams of a sample were crushed to a size smaller than 100 μm. Each gram of the crushed sample was mixed with 12·00 g of $Li_2B_4O_7$ in a platinum crucible and melted at 1300°C for 15 min. After melting, the substance was cast and subsequently measured on an ARL ADVANT'X series Sequential XRF IntelliPower (Thermo).

2.7. Mössbauer spectroscopy

To investigate the redox state of iron in the glassy phase, Mössbauer spectroscopy was carried out on

a powdered glass sample melted at 1300°C for 40 min. A constant acceleration spectrometer with a ^{57}Co source in rhodium was used. The spectrometer was calibrated using an α-Fe foil at room temperature.

3. Results and discussion

The melts produced at 1300°C for 10 and 20 min contain white undissolved grains with a size of 2–5 mm. Since the grains are not dissolved, a separation of the grains from the glass matrix is feasible, which allows compositional analysis of the grains by means of x-ray fluorescence. The undissolved grains in the glass could potentially be any of the three rocks in the glass batch: basalt, dolomite and bauxite. XRF analysis shows that the undissolved grains contain 51·9 mol% CaO and 44·3 mol% MgO, indicating that the undissolved grains are dolomite. The dolomite used in this work has a rather high MgO content. A previous study has shown that dolomites of high MgO content are less suitable for container glass production than dolomites of lower MgO content.[17] The high melting point of dolomite is believed to be responsible for its limited dissolution in the glass melt after retention times of 10 and 20 min at 1300°C. A retention time of 40 min at 1300°C is sufficient for dissolving most of the dolomite grains in the glass melt. The presence of undissolved dolomite grains in the glass causes fracture of the glass during sample preparation for the striae characterisation. Consequently, only the glass subjected to a retention time of 40 min at 1300°C can be analysed with respect to striae, because the samples subjected to melting retention time of 10 and 20 min at 1300°C are so brittle that samples with sufficient dimensions for image analysis could not be obtained.

During the casting process, the formation of a separate metallic liquid phase is observed on the bottom of the melting crucible. The metallic phase is believed to be predominantly iron that is created upon reduction of iron oxide by graphite doped into the SiC crucible. The presence of the metallic iron phase suggests that only ferrous iron is found in the glassy phase and this is verified by the Mössbauer measurements (Figure 2). Since only a Fe^{2+} duplet is observed in the Mössbauer spectrum of the glass melted at 1300°C, the content of ferric iron must be lower than the detection limit of the Mössbauer apparatus, i.e. 3% of the total iron content. The iron redox equilibrium is shifted towards the reduced state with increasing melting temperature.[18–21] Therefore, ferrous iron accounts for at least 97% of the total iron content in the glasses produced at temperatures above 1300°C. It is observed that the amount of metallic iron precipitated at the bottom of the crucible is increased when the melting temperature exceeds 1300°C. To verify this observation, the FeO content is measured in the glass phase for samples melted

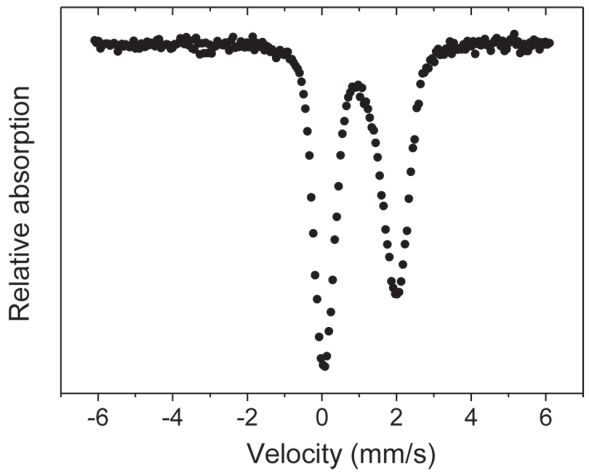

Figure 2. Mössbauer spectrum of the glass sample melted at 1300°C for 40 min. The duplet in the spectrum arises from Fe^{2+}

at different temperatures for 40 min as samples with the longest retention time are closer to redox equilibrium (Figure 3). The iron oxide content in the melt decreases with increasing melt temperature. The iron reduction removes network modifying Fe^{2+} ions from the glass melt, which increases the melt viscosity.[22] Therefore, the actual viscosity of the melt is somewhat higher than that calculated from the batch composition in Section 2.1. Based on the difference between the iron content in the batch and in the actual melt (Figure 3), the concentration of the other components is recalculated according to the overall changes of glass compositions due to the iron precipitation (Table 2). From the Bottinga–Weill model,[15] the viscosities of the melt at 1300, 1350, 1400 and 1450°C, which are corrected by considering iron precipitation, are calculated to be 5·9, 3·5, 3·0 and 1·9 Pa s, respectively. Hence the viscosities of the actual

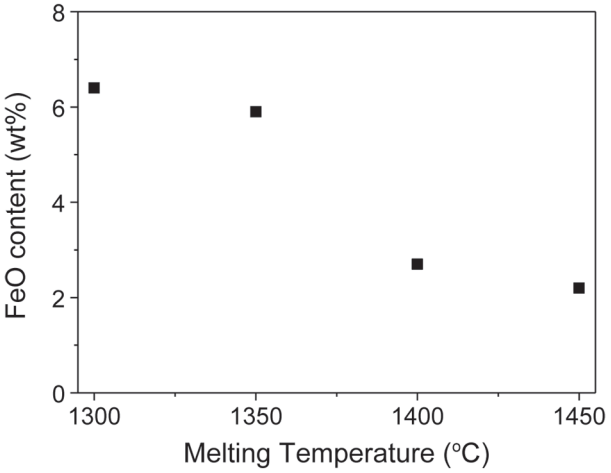

Figure 3. FeO content determined by means of x-ray fluorescence in the glasses melted at various temperatures for 40 min. All of the iron is present as FeO according to the Mössbauer measurements. In the batch, the FeO content is 8·1 wt%

Table 2. Chemical composition in wt% of the melts produced at the four melt temperatures with a retention time of 40 min. The chemical compositions are determined by measurement of the iron content of the melt and subsequently rescaling of the concentration of the other components based on the extent of metallic iron formation. All iron is reported as Fe_2O_3 to make the compositions comparable to those in Table 1. The viscosity of the melt at the actual melt temperature is calculated from the Bottinga–Weill model[15]

Melting temp (°C)	*SiO_2*	*Al_2O_3*	*TiO_2*	*Fe_2O_3*	*CaO*	*MgO*	*Na_2O*	*K_2O*	*η (Pas)*
1300	41·0	18·1	1·6	8·5	18·6	8·5	2·6	0·9	5·9
1350	41·3	18·2	1·6	7·7	18·8	8·6	2·6	0·9	3·5
1400	43·2	19·0	1·7	3·5	19·6	9·0	2·7	1·0	3·0
1450	43·3	19·1	1·7	3·0	19·8	9·0	2·7	1·0	1·9

melt are higher than those of the melt corresponding to the batch composition (4·9, 2·7, 1·8 and 1·1 Pas).

A visual inspection of the glass samples subjected to different melting temperatures shows that both bubbles and striae are present in the glasses (Figure 4). The samples produced at 1300°C in the SiC crucible and at 1400°C in the Cr_2O_3 coated SiC crucible appear more striated than melts produced at 1350, 1400 and 1450°C in the SiC crucible. Melts produced in the Cr_2O_3 coated SiC crucible experienced weaker reducing conditions in the melt compared to those produced in the uncoated SiC crucible. From a visual inspection of the images in Figure 4, it is difficult to find differences in stria content in the glasses melted at different temperatures in the SiC crucible.

To quantify the striations in the glasses, line scans are conducted on acquired images, which provide the same information as conventional transmission measurements, but at a data acquisition rate that is orders of magnitude faster. Chemical striae display a gradual increase or decrease in the concentration of one or more species from the glass matrix towards the centre of the stria. This nature of the chemical fluctuations in the glass causes a harmonically oscillating stria concentration across the glass as explained in detail elsewhere.[12] Due to the harmonic oscillating motion of the stria concentration, the stria concentrations determined during each line scan are subjected to a Fourier transform. From the Fourier transform the stria intensity (amplitude) as a function of reciprocal dimension (frequency) is obtained. The stria intensity integrated from large to small dimensions is plotted against dimension for the glasses melted for 10, 20 and 40 min in the SiC crucible (Figure 5). For each glass, 500 line scans with a length of 2500 pixels are conducted on random spots on the glass. Since five samples are prepared from each melt, every curve in Figure 5 is based on optical transmission measurement of 6 250 000 spots each with a size of 7·9×7·9 μm^2. Most samples show the largest increase in integral intensity at dimensions above 200 μm, i.e. striae larger than 200 μm constitute a large part of the stria intensity in the glasses. From the integral intensity it cannot be clarified whether large stria intensity originates from several weak striae or a few intense ones. As either the melting temperature is increased or retention time prolonged, the integral intensity decreases.

To obtain a quantitative measure of the total stria content in the glasses, the integral intensity at 20 μm (I_{20}) is determined. From the applied image acquisition resolution of 3200 dpi, one pixel on the acquired images has an area of 7·9×7·9 μm^2. As any fluctuation requires at least two points, a detectable fluctuation in the stria concentration must at least occur over a length of 16 μm. Consequently, the integral intensity

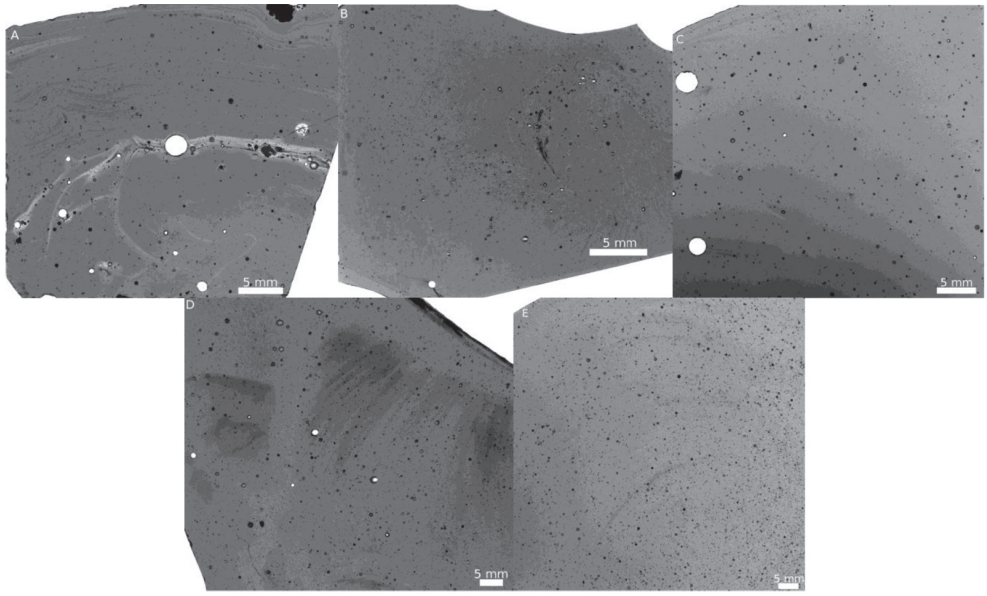

Figure 4. Scanned grey tone images of samples melted for 40 min at (A) 1300°C in a SiC crucible, (B) 1350°C in a SiC crucible, (C) 1400°C in a SiC crucible, (D) 1400°C in a SiC crucible coated with Cr_2O_3 refractory paste and (E) 1450°C in a SiC crucible

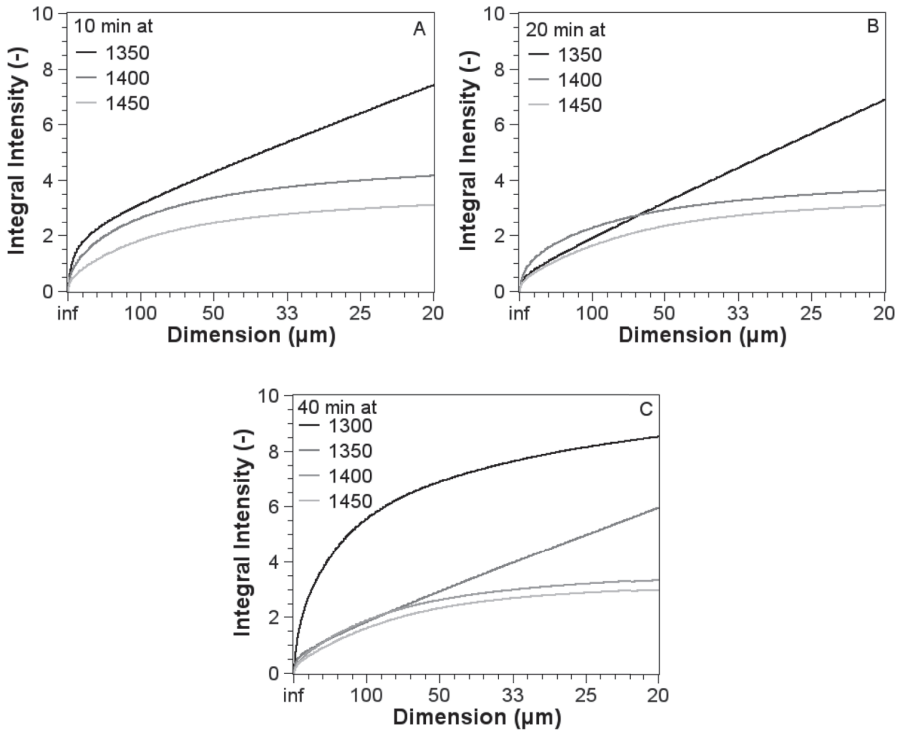

Figure 5. Integrated intensity as a function of dimension for glasses melted for (A) 10 min, (B) 20 min and (C) 40 min. The integral intensity is obtained by integration of the Fourier transform spectra of line scans. 500 randomly oriented lines scans are performed on each glass and 5 glasses of each melt are investigated. It was not possible to produce samples for striae characterisation from melts produced at 1300°C for 10 and 20 min due to undissolved raw materials in the samples

at 20 μm is considered to be a measure of the total detectable stria content in the glass. The total stria content (I_{20}) for the different glasses melted in SiC crucible is given in Figure 5. As expected Figure 5 shows that the total stria content decreases with increasing retention time or melting temperature.

The impact of melting temperature on the glass homogeneity (in terms of total stria content, I_{20}) seems to reach a threshold around 1450°C, i.e. furthermore increase of the melting temperature is only expected to produce a minor improvement in the stria equilibration rate. In other words, the reduction of the dimension of the striae and the decrease of the chemical gradient between the striae and the surrounding glass matrix is expected to display little dependence on temperature at temperatures above 1450°C. With the setup used here it has not been feasible to produce melts at 1500°C. In general, the effect of a 50°C increase in the melting temperature on the stria content of the melt is larger than a quadrupling the retention time from 10 to 40 min. The small impact of retention time on stria equilibration has its physical origin in the diffusion controlled equilibration of striae. The dependence of retention time, t_i, on the diffusion length, x_i, of component i, is given by

$$x_i = c_i \sqrt{t} \qquad (2)$$

where c_i is a component specific constant that increases with decreasing viscosity, i.e. increasing temperature of the melt. Stria equilibration occurs via diffusion at both interfaces between the striated domain and the surrounding melt, which implies that complete elimination of a stria in the melt requires that the diffusion length is at least half of the stria dimension. From Equation (2) it is seen that quadrupling the retention time provides a doubling of the diffusion length. The effect of melting temperature on the diffusion length is more complex than that of the retention time. Stria can be caused by concentration differences of various components, and hence, the diffusion of several species proceeds simultaneously during the melting process. As the influence of melting temperature on each c_i is unknown, the influence of melting temperature on the diffusion length cannot be estimated. The effect of retention time on the diffusion length is to a minor extent influenced by the reduction of Fe^{2+} to Fe^0. The reduction removes the network modifying Fe^{2+} from the glass network,[22] and hence increases the melt viscosity, i.e. c_i in Equation (2) decreases. The influence of retention time on the iron reduction is, however, small as the iron oxide content decreases from 6·8 to 5·9 wt% when the retention time is prolonged from 10 to 40 min at 1350°C. In addition to gradients in the chemical composition, striae can be created by local oxidation state fluctuations of iron in the melt. The formation mechanism of redox induced striae is different from that of the striae caused by chemical gradients. In this work, we focus on the kinetics of elimination of the compositional gradient.

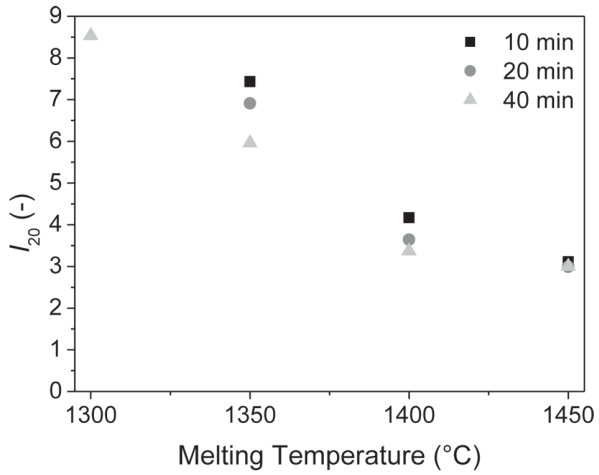

Figure 6. Integral intensity at 20 μm (I_{20}) as a function of melting temperature

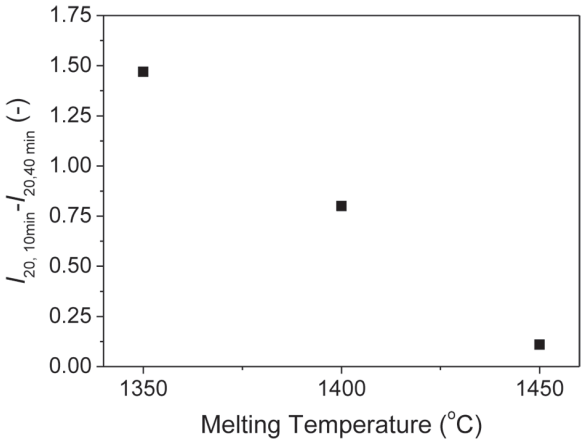

Figure 7. The difference in homogeneity of a melt produced in a SiC crucible at a given temperature for 10 and 40 min as a function of melting temperature. The difference in homogeneity is determined as that in total striae concentration (I_{20}) between melts homogenised for 10 and 40 min

Interestingly, the difference in glass homogeneity between a retention time of 10 and 40 min decreases when the melting temperature is elevated (Figure 6). To quantify the effect of a prolonged retention time on homogeneity at different temperatures, the difference between I_{20} at 10 min and I_{20} at 40 min is determined (Figure 7). The difference in stria content between a glass melted for 10 min and 40 min seems to show a linear decrease with increasing melting temperature. The trend can partly be explained by the experimental procedure. During the melting experiments, the temperature of the raw materials is allowed to equilibrate at 1100°C and thereafter the crucible is heated at a rate of 20°C/min to the target temperature. Since most raw materials are dissolved at 1300°C, homogenisation occurs during the heating process from 1300 to 1350, 1400 or 1450°C. Therefore, at higher melting temperatures, the extent of striae equilibration during the heating process increases. An increase in the retention time from 10 to 40 min, doubles the diffusion length in the melt (Equation (2)). The increase in diffusion length enables the equilibration of larger striae, yet only a limited improvement in homogeneity is seen by prolonging the retention time at high melting temperatures. This can be explained by the following two aspects. First, at higher melting temperatures, the easily eliminable striae, i.e. small striae enriched/depleted in quickly diffusing species, are equilibrated during the heating process and the first 10 min of retention. Second, this leaves large striae and striae enriched/depleted in slowly diffusing species in the melt and therefore the effect of retention time on the stria equilibration is smaller than expected. For a soda–lime–silica melt, the diffusion rate has been found to vary by more than two orders of magnitude, depending on the type of diffusing species in question.[23] Since the iron-bearing calcium aluminosilicate melt investigated in this study is produced from a multicomponent batch, striae with different chemical origins are likely to exist, i.e. striae with quickly and slowly diffusing species exist in the melt. At low melting temperatures, even striae caused by quickly diffusing species require 40 min to equilibrate and therefore a rather large effect of the retention time on the stria content is observed at low melting temperatures. At higher temperatures, elimination of striae enriched/depleted in quickly diffusing species occurs within 10 min, whereas gradients in slowly diffusing species persist. Therefore, the difference in homogeneity between samples melted for 10 or 40 min is lower at 1450°C than that at 1350 and 1400°C. Hence, complete elimination of striae in a glass melt with striae enriched/depleted in slowly diffusing species is difficult.

To explore the effect of the melt viscosity on the homogenisation rate of the melt without changing the melt temperature, the inner surface of the crucible is covered with a Cr_2O_3 refractory paste. As the paste prevents contact between the glass melt and the reducing crucible, the redox conditions in the melt are shifted to a more oxidised state and the extent of iron reduction of the melt is reduced when the Cr_2O_3 paste is applied. The change in the redox state of the melt is reflected by a shift in the iron redox ratio in the glass network. The redox state of iron is important to the viscosity of the glass melt as Fe^{2+} acts as a network modifier in the glass network whereas Fe^{3+} is a network former.[22] Therefore, a shift of iron from the ferrous to the ferric state implies a conversion of network modifier to network former, which increases the viscosity of the melt. The total iron oxide content is higher for the melt produced in Cr_2O_3 coated crucible than in the melt produced in the SiC crucible. Further, the ferric iron constitutes about 60% of the iron content in the melt produced in the Cr_2O_3 coated crucible.[24] Hence, utilisation of the Cr_2O_3 paste increases the total iron oxide content in the melt and alters the iron redox ratio. Theoretical

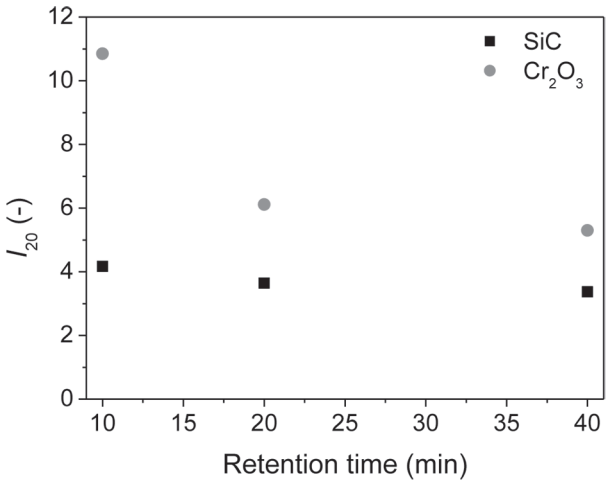

Figure 8. The total stria content (I_{20}) against the retention time for melts produced in a SiC crucible (SiC) or a SiC crucible covered with Cr_2O_3 (Cr_2O_3) refractory paste produced at 1400°C

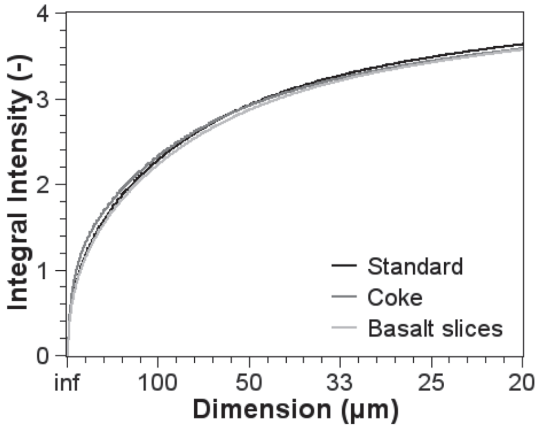

Figure 9. Integral intensity as a function of dimension for melt produced in a SiC crucible at 1400°C for 20 min. 'Coke' denotes a melt produced from a batch with 2 wt% coke. For 'Basalt slices' the batch contained larger basalt slices as distinct from the smaller basalt pieces used for the other batches

quantification of these two effects on the melt viscosity is difficult, however during casting of the melts it was clear that the melts produced in the Cr_2O_3 coated crucible had a higher viscosity than those produced in the SiC crucible. Besides affecting the viscosity of the melt, precipitation of iron releases the oxygen that is bonded to the ferrous ion in the glass network. The released anionic oxygen can react with graphite in the crucible surface layer, and this creates CO and CO_2.[25] Due to the buoyancy force, the CO and CO_2 containing bubbles ascend to the surface of the melt. As the bubbles ascend, they exert shear forces on the melt, which convert large striae to smaller ones.[26] The conversion of larger striae to smaller ones enhances the rate of stria elimination in the melt,[26] i.e. bubble formation can also reduce the stria content of the melt to some extent. The homogeneity of glasses produced at 1400°C in thr SiC crucible is compared with that of glasses produced at 1400°C in the Cr_2O_3 coated SiC crucible with respect to the total stria content in the melts (I_{20}) (Figure 8). I_{20} is larger for the glasses produced in the Cr_2O_3 covered crucible, i.e. glasses produced in the crucible covered with Cr_2O_3 paste are more inhomogeneous than those produced in SiC crucible. To determine whether the Cr_2O_3 dissolves in the glass melt and creates Cr_2O_3 enriched striae, the Cr_2O_3 content in the glass is measured by means of XRF. For glasses melted for 10, 20 and 40 min, the Cr_2O_3 content is 0·11, 0·19 and 0·86 wt%, respectively. As the largest difference in I_{20} between the two melting conditions occurs in the glasses with the lowest Cr_2O_3 content, it is inferred that the extent of Cr_2O_3 in the melt is below the limit where it affects the stria characterisation. Therefore, the difference in homogeneity between the melts produced in the two crucibles is ascribed to the viscosity change caused by the shift in the redox state of iron. The compositional change caused by iron reduction is found to increase the viscosity by about 1 Pa s for the four used melting temperatures, but the viscosity difference between the melts produced in the two crucibles is considerably larger than 1 Pa s. Therefore, it can be inferred that the viscosity difference between the two melts is mainly induced by the variation in the redox state of iron in the melt. At a fixed chemical composition the diffusion rate is inversely proportional to viscosity, i.e. c_i in Equation (2) is lowered upon increase of viscosity. The decrease of the diffusion length caused by the viscosity increase explains the lower homogeneity of the more viscous melts. An increase in the viscosity of the melts produced in the Cr_2O_3 coated crucible has been observed during the casting process. The effect of viscosity on the homogenisation rate demonstrates that besides affecting the properties of the final glass product,[27–30] the redox state of polyvalent elements has an influence on the melting and casting process of glasses. Casting of glass products is performed at a certain viscosity. When the redox state of polyvalent elements varies, the casting temperature should be adjusted in order to keep the viscosity constant. As an example, the viscosity of an iron bearing soda silica melt at 1430°C has been reported to decrease from 14 to 10 Pa s when ferric ions are reduced to ferrous ones.[31]

According to the above mentioned findings, enhancement of the oxidising conditions decreases the homogeneity of the melt. Now the question is whether enhancement of the reducing conditions of a melt (e.g. conditions more reducing than those of the as-obtained SiC crucible) influences the homogeneity of the melt. To answer this question, we add 2 wt% of coke grains to a batch melted at 1400°C for 20 min in order to explore whether reducing grains uniformly distributed in the melt create different conditions than those of the crucible surface. The integral intensity of the striae in the melt produced from the coke containing batch is similar to that produced from a

batch without coke (Figure 9). As demonstrated by Mössbauer spectroscopy (Figure 2), the SiC crucible provides a strongly reducing environment as no ferric iron can be detected in the glass structure. Since the reducing power of the crucible is sufficient to eliminate Fe^{3+} in the glass network, the addition of coke does not further influence the redox state of the iron in the glass network. Thus, the stria content is independent of the addition of coke to the batch.

To investigate the chemical origin of the striae in the melt, the size of the basalt pieces in the batch is increased from ~ 8 cm^3 in the normal batches to ~140 cm^3. The increased size of the basalt pieces requires a larger diffusion length to fully eliminate their concentration gradient in the melt. The stria intensity in the melt produced from a batch with large basalt slices is similar to that in the standard melt (Figure 9). Therefore, the striae in the glass samples are not caused by the basalt in the batch. Consequently, one or more of the raw material grains in the briquette (basalt, dolomite and bauxite) must be the main origin of the striations in the glasses. This is evidenced by the presence of the undissolved dolomite grains found after a retention time of 20 min at 1300°C. As dolomite is the last raw material to dissolve in the melt, it is likely that concentration gradients in Ca^{2+} and Mg^{2+} exist in the melt. An earlier study has found that the limestone grain size influences the concentration gradient of Ca^{2+} in silicate melts,[32] i.e. the limestone is the origin of the chemical striae. This gives a further indirect indication that at least some of the striae in the glasses produced in this work originate from concentration gradients in Ca^{2+} and Mg^{2+}, i.e. from dolomite.

4. Conclusions

The homogeneity of iron-bearing calcium aluminosilicate glasses with a basalt-like composition is characterised with respect to the stria content in the glasses by means of image analysis. The stria intensity can be lowered by increasing the melting temperature and/or the retention time. The melting temperature has a larger influence on the homogenisation of the melt than the retention time. Besides the melting temperature and retention time, the redox state of iron has impact on the homogenisation rate of the melt. A conversion of Fe^{2+} to Fe^{3+} leads to an increase in the melt viscosity and a concomitant decrease in the homogenisation rate. The striae in the melt could originate from gradients in the concentration of Ca^{2+} and Mg^{2+} due to the presence of dolomite in the glass batch.

Acknowledgements

We thank R. Keding, M. Solvang, T. Madsen, V. Boffa and L. Wybrandt for assistance during glass casting and for useful discussions. This work is financially supported by Rockwool International A/S.

References

1. Abrams, M. B. & Green, D. J. Prediction of crack propagation and fracture in residually stressed glass as a function of the stress profile and flaw size distribution. *J. Eur. Ceram. Soc.*, 2006, **26**, 2677–84.
2. Sheu, T. S. & Green, D. J. Fracture strength of ion-exchange silicate-containing dental glass ceramics. *J. Mater. Sci.*, 2007, **42**, 2064–9.
3. Lund, M. D. & Yue, Y. Z. Fractography and tensile strength of glass wool fibres. *J. Ceram. Soc. Jap.*, 2008, **116**, 841–5.
4. Capps, W., Schaeffer, H. A. & Cronin D. J. The effect of striae on the strength of glass. *J. Am. Ceram. Soc.*, **63**, 570–3.
5. Hogerl, K. & Frischat, G. H. Homogenisation of glass melts by bubbling on a laboratory scale. *Glastech. Ber.*, 1994, **67**, 145–50.
6. Hermans, J. & Beerkens, R. The dissolution of cords in molten glass. *Ceramics-Silikaty*, 1999, **43**, 147–50.
7. Bange, K., Müller, H. & Strubel, C. Characterisation of defects in glasses and coatings on glasses by microanalytical techniques. *Microchim. Acta*, 2000, **132**, 493–503.
8. Stroud, J. S. Striae quality grades for optical glass. *Opt. Eng.*, 2003, **42**, 1618–24
9. Kemeklis, L., Balandis, A. & Vaitskyalenis, G. Reasons for the formation of cords in melting electrovacuum strontium glass in a flame tank glassmelter of new design. *Glass Ceram.*, 2004, **61**, 248–51.
10. Ohashi, Y., Kushibiki, J.-I., Arakawa, M. & Suzuki, K. Experimental study for evaluating striae structure of TiO_2–SiO_2 glasses using the line-focus-beam ultrasonic material characterisation system. *Jpn. J. Appl. Phys.*, 2006, **45**, 6445–51.
11. Krieger, U., Halbedel, B., Hülsenberg, D. & Thess, A. Electromagnetic effects on glass melt flow in crucibles. *Glass. Technol.: Eur. J. Glass. Sci. Technol. A*, 2008, **49** (1), 33–40.
12. Jensen, M., Keding, R. & Yue, Y. Z. Quantification of chemical striae in inorganic melts and glasses through picture processing. *J. Am. Ceram. Soc.*, 2010, **93**, 2705–12.
13. Jensen, M., Keding, R., Poschwatta, H. H., Fjendbo, S. & Yue, Y. Z. Effect of bubbles on the characterisation of striae in glasses. *Glass Technol.: Eur. J. Glass Sci. Technol. A*, 2010, **51** (4), 147–52.
14. Jensen, M., Zhang, L., Keding, R. & Yue, Y. Z. Homogeneity of inorganic glasses: Quantification and ranking. *Int. J. Appl. Glass Sci.*, 2011, **2**, 137–43.
15. Bottinga, Y. & Yan, D. F. The viscosity of magmatic silicate liquids; a model calculation. *Am. J. Sci.*, 1972, **272**, 438–75.
16. Abramoff, M. D., Magelhaes, P. J. & Ram, S. J. Image processing with ImageJ. *Biophoton. Int.*, 2004, **11**, 36–42.
17. Dagounaki, C., Sikalidis, C., Kassoli-Fournaraki, A. & Tsirambides, A. An evaluation of alternative sources of carbonate rocks for glass making from the Kozani region, NW Macedonia, Greece. *Glass Technol.: Eur. J. Glass Sci. Technol. A*, 2009, **50** (5), 253–7.
18. Dingwell, D. B. & Brearley, M. Melt densities in the CaO–FeO–Fe_2O_3–SiO_2 system and the compositional dependence of the partial molar volume of ferric iron in silicate metls. *Geochim. Cosmochim. Acta*, 1988, **52**, 2815–25.
19. Lange, R. A. & Carmichael, I. S. E. Ferric-ferrous equilibria in Na_2O–FeO–Fe_2O_3–SiO_2 melts: Effects of analytical techniques on derived partial molar volumes. *Geochim. Cosmochim. Acta*, 1989, **53**, 2195–204.
20. Magnien, V., Neuville, D. R., Cormier, L., Roux, J., Hazemann, J.-L., de Ligny, D., Pascarelli, S., Vickridge, I., Pinet, O. & Richet, P. Kinetics and mechanisms of iron redox reactions in silicate melts: The effects of temperature and alkali cations. *Geochim. Cosmochim. Acta*, 2008, **72**, 2157–68.
21. Borisov, A. & McCammon, C. The effect of silica on ferric/ferrous ratio in silicate melts: An experimental study using Mössbauer spectroscopy. *Am. Mineral.*, 2010, **95**, 545–55.
22. Mysen, B. O. & Richet, P. *Silicate Glasses and Melts. Properties and Structure*. Elsevier, Amsterdam, 2005.
23. Rüssel, C. Self diffusion of polyvalent ions in a soda-lime-silica glass melt. *J. Non-Cryst. Solids*, 1991, **134**, 169–75.
24. Jensen, M., Zhang, L. & Yue, Y. Z. Probing iron redox state in multi-component glass by XPS. *Chem. Geol.*, (under review).
25. Jensen, M., Keding, R. & Yue, Y. Z. Bubble formation in basalt-like melts. *Glass Technol.: Eur. J. Glass Sci. Technol. A*, 2011, **52** (4), 127–35.
26. Jensen, M. & Yue, Y. Z. Effect of stirring on striae in glass melts. *J. Non-Cryst. Solids*, in press.
27. Mekki, A. & Ziq, Kh. A. Magnetic properties of a SiO_2–Na_2O–Fe_2O_3 glass and glass ceramic. *J. Magn. Magn. Mater.*, 1998, **189**, 207–213.
28. Khonthon, S., Morimoto, S., Arai, Y. & Ohishi, Y. Redox equilibrium and NIR luminescence of Bi_2O_3-containing glasses. *Opt. Mater.*, 2009, **31**, 1262–8.
29. Lund, M. D., Yue, Y. Z. & Lybye, D. Impact of the oxidation state of iron on the tensile strength of stone wool fibres. *Glass. Technol.: Eur. J. Glass. Sci. Technol. A*, 2010, **51** (3), 97–102.
30. Srikumar, T., Srinvasa Rao, Ch., Gandhi, Y., Venkatramaiah, N., Ravikumar, V. & Veeraiah, N. *J. Phys. Chem. Solids*, 2011, **72**, 190–200.
31. Dingwell, D. B. & Virgo, D. The effect of oxidation state on the viscosity of melts in the system Na_2O–FeO–Fe_2O_3–SiO_2. *Geochim. Cosmochim. Acta*, 1987, **51**, 195–205.
32. Chopinet, M. H., Gouillart, E., Papin, S. & Toplis, M. J. Influence of limestone grain size on glass homogeneity. *Glass Technol.: Eur. J. Glass. Sci. Technol. A*, 2010, **51** (3), 116–22.